Iğdır Üniversitesi Fen Bilimleri Enstitüsü Dergisi, 13(2), 872-888, 2023
Journal of the Institute of Science and Technology, 13(2), 872-888, 2023

ISSN: 2146-0574, eISSN: 2536-4618

Biology **DOI: 10.21597/jist.1187616**

Research Article

Received: 12.10.2022 **Accepted: 11.01.2023**

To Cite: Akbaba E. & Karataş, D. (2023). Phytochemicals of Hibiscus sabdariffa with Therapeutic Potential against SARS-CoV-2: A Molecular Docking Study. *Journal of the Institute of Science and Technology*, 13(2), 872-888.

Phytochemicals of Hibiscus sabdariffa with Therapeutic Potential against SARS-CoV-2: A Molecular Docking Study

Emel AKBABA[1], Deniz KARATAŞ[2*]

Highlights:

- The phytochemicals of Hibiscus sabdariffa could be alternatives to remdesivir and nelfinavir.
- The most favorable ligands are found to be caffeoylshikimic acid, chlorogenic acid, and cianidanol for 3CLpro.
- Strong binding affinities of nicotiflorin, chlorogenic acid, and quercetin pentosylhexoside for PLpro were monitored.
- The driving forces for the interactions between the ligands and the receptors of 3CLpro and PLpro were found to be H-bonds and van der Waals interactions.
- The inhibition constant values decrease as the binding energies fall.

ABSTRACT:

In this study, the possible interactions of 17 phytochemicals that were reported as the most abundant biomolecules of *Hibiscus sabdariffa*, including many organic acids as well as catechin and quercetin derivatives, with $3CL^{pro}$ and PL^{pro} proteases of SARS-CoV-2 have been investigated via molecular docking. Caffeoylshikimic acid/$3CL^{pro}$ showed the lowest binding energy (-7.72 kcal/mol) with seven H-bonds. The second-lowest binding energy was computed in the chlorogenic acid/$3CL^{pro}$ complex (-7.18 kcal/mol), which was found to form 6 H-bonds. Also, low binding energies of cianidanol (-7.10 kcal/mol), cryptochlorogenic acid (-6.67 kcal/mol), and kaempferol (-6.82 kcal/mol) were calculated to $3CL^{pro}$ with several H-bond interactions. Nelfinavir (-10.16 kcal/mol) and remdesivir (-6.40 kcal/mol), which have been used against COVID-19, were obtained to have low binding energies to $3CL^{pro}$ with 3 H-bond formations each. On the other hand, the nicotiflorin/PL^{pro} complex, which had the lowest binding energy (-7.40 kcal/mol), was found to have only 1 H-bond interaction. The second-lowest binding energy was reported in chlorogenic acid/PL^{pro} (-7.20 kcal/mol), which was found to possess four H-bonds. On the other hand, epigallocatechin gallate/PL^{pro}, which was shown to have a -5.95 kcal/mol binding energy, was found to form 8 H-bond interactions. Furthermore, the quercetin pentosylhexoside/PL^{pro} complex was monitored to have low binding energy (-6.54 kcal/mol) with 9 H-bonds, which stands as the highest number of H-bonds in all complexes. Therefore, several molecules of *Hibiscus sabdariffa* were found to have strong binding affinity to the main proteases of SARS-CoV-2. This study suggests many compounds, including caffeoylshikimic acid and nicotiflorin, to inhibit $3CL^{pro}$ and PL^{pro} activities. As a result, numerous chemicals derived from *Hibiscus sabdariffa* have the potential to be employed therapeutically against SARS-CoV-2 infection.

Keywords:

- $3CL^{pro}$
- *Hibiscus sabdariffa*
- molecular docking
- PL^{pro}
- SARS-CoV-2

[1] Emel AKBABA (**Orcid ID:** 0000-0003-4915-5153), Kirikkale University, Faculty of Medicine, Department of Medical Biology, Kırıkkale, Türkiye

[2] Deniz KARATAŞ (**Orcid ID:** 0000-0002-8176-4883), Manisa Celal Bayar University, Bioengineering Department,Yunusemre, Manisa, 45140, Türkiye

***Sorumlu Yazar/*Corresponding Author**: Deniz KARATAŞ, e-mail: deniz.karatas@cbu.edu.tr

INTRODUCTION

In March 2020, the World Health Organization (WHO) proclaimed a pandemic named "Coronavirus disease of 2019" (COVID-19). Since then, the number of new instances has increased dramatically. The COVID-19 infection may present with symptoms such as fever, coughing, and respiratory illness. Certain critically ill patients may develop pneumonia and/or trouble breathing, which may progress to multi-organ failure and death (Deb et al., 2022).

Seven coronaviruses (CoVs) have been linked to human illnesses so far. Four of these CoVs, known as a non-severe acute respiratory syndrome (SARS)-like CoVs, cause mild infections and are worldwide endemic, but three highly pathogenic CoVs (SARS-CoV-1, MERS, and SARS-CoV-2) may result in fatal disease (Vlachakis et al., 2020). As a result of the SARS-CoV-2 pandemic, which has resulted in COVID19, the healthcare system has been placed under considerable strain (Takeuchi et al., 2021).

CoVs are an enclosed virus family with a large (26-32 kilobases) positive-sense single-stranded RNA coding for 29 proteins. The SARS-CoV-2 genome has an overall 80% nucleotide identity with SARS-CoV, and the main proteases of these viruses have more than 90% amino acid sequence identity (Ghosh et al., 2021). They are found in a broad variety of animals and may infect humans, particularly affecting the respiratory, hepatic, and gastrointestinal systems, and even the central nervous systems (Shawky et al., 2020).

Researchers from all around the globe have been experimenting with various methods for limiting viral reproduction. Among the several targets, two proteases, papain-like protease (PL^{pro}, a domain within Nsp3) and chymotrypsin-like main protease ($3CL^{pro}$, corresponding to Nsp5), are critical for viral replication and are thus regarded as major druggable targets. The proteolytic actions of PL^{pro} and $3CL^{pro}$ produce various non-structural proteins (NSPs), such as RNA-dependent RNA polymerase and helicase, that are required in the viral life cycle (Chen et al., 2021).

PL^{pro} is a domain of Nsp3—a large multidomain protein that is an essential component of the replicase-transcriptase complex (RTC). The PL^{pro} exhibits multiple proteolytic activities along with many other functions. The enzyme is involved in host cell immune suppression through the inactivation of TANK-binding kinase 1 (TBK1) and the inhibition of Toll-like receptor 7 (TLR7) and the NF-kappa B signaling pathways (Osipiuk et al., 2021). SARS and SARS-CoV-2 share a PL^{pro} sequence identity of 83% (Solnier et al., 2021). Therefore, it is considered an excellent target for the creation of broad-spectrum inhibitors (Amin et al., 2022).

$3CL^{pro}$, also known as the main protease (M^{pro}), functions as a cysteine protease to cleave the polyproteins at 11 positions into individual polypeptides essential for viral replication and transcription with stringent substrate specificity (Mody et al., 2021). Structure and activity analysis revealed that the active site of $3CL^{pro}$ contains a catalytic dyad. The $3CL^{pro}$ protease of SARS-CoV-2 shares over 95% of its sequence similarity with that of SARS-CoV (Kumar et al., 2020). Given its important role in CoV replication, $3CL^{pro}$ is considered a prominent drug target of antiviral therapy (Chen et al., 2021).

Several drugs have been screened to inhibit the replication of SARS-CoV-2 so far, including anti-viral medications used for other infections, synthesized chemicals, and natural phytochemicals (Agrawal et al., 2022). The natural products with promising inhibitory actions against SARS-CoV-2 are mainly flavonoids, terpenoids, and alkaloids, mostly comprising flavonoid skeletons (Omrani et al., 2020). Flavonoids are known to possess anti-inflammatory properties in viral illnesses, promoting the host immune response (Dong et al., 2014). Flavonoids were also reported to reduce overwhelming

inflammatory responses, which are commonly linked with greater fatality rates in SARS-CoV-2 infections (McKee et al., 2020).

Hibiscus L. species (red sorrel, Malvaceae) has been traditionally used as food, in herbal drinks, in beverages, as a flavoring agent in the food industry, and as herbal medicine. Including more than 300 species, *Hibiscus* is widely cultivated in both tropical and subtropical regions (Da-Costa-Rocha et al., 2014). Many health benefits of flavonoids and phenolic acids of *Hibiscus* species have been reported, such as antihypertensive, antibacterial, antidiabetic, antioxidant, nephroprotective, hepatoprotective, renal/diuretic effects, and anti-cholesterol effects (Hapsari et al., 2021). *H. sabdariffa* is well known and widely consumed as a colorant in herbal tea preparations. It is very popular and cultivated in some parts of North Africa, especially in Egypt and Sudan. The samples of *H. sabdariffa* are sold on the market in many countries, including Europe. Through the use of molecular docking, the potential interactions of the main phytochemicals in *H. sabdariffa* with the $3CL^{pro}$ and PL^{pro} proteases of SARS-CoV-2 were investigated in this study.

MATERIALS AND METHODS

In this study, the interactions of the main phytochemicals of *H. sabdariffa* and antiviral medications with corona viral proteases were carried out via molecular docking. The structures of the ligand molecules are shown in Figure 1. The compounds and antiviral drugs were selected as the ligands, while proteases were selected as the receptors. The polar hydrogens and their charges were assigned to the ligands. Then ligands were added to the receptors one by one via Autodock *v*4.2.6 so that the interactions were computed independently (Morris et al., 2009). The PDB IDs of the receptors were taken from the RCSB protein databank as 5R7Y entry (Douangamath et al., 2020) for $3CL^{pro}$ and 6W9C entry for PL^{pro} (Osipiuk et al., 2021).

The RCSB PDB server revealed that the 3C-like proteinase of SARS CoV-2 has a resolution of 1.65 Å, a total structural weight of 34.37 kDa, and a modeled residue number of 304 (Figure 2a). The molecule has one unique protein chain with a sequence length of 306 (Douangamath et al., 2020) . The enzyme's active site contains a catalytic dyad (HIS41, CYS145) where a cysteine residue acts as a nucleophile in the proteolytic process and a histidine residue acts as the general acid base (Douangamath et al., 2020; Nouadi et al., 2021). On the other hand, the papain-like protease of SARS CoV-2 has a resolution of 2.70 Å, a total structural weight of 107.81 kDa, and a modeled residue number of 926 (Figure 2b). The molecule has 3 chains: A, B, and C, with a sequence length of 317, which has a reported "thumb-palm-fingers" architecture (Osipiuk et al., 2021). The active site of PL^{pro} has been shown to have a catalytic triad composed of CYS111, HIS272, and ASP286 (Osipiuk et al., 2021).

The visualizer of the Autodock *v*4.2.6 was used to remove the explicit water molecules from the receptors. Then, Zn^{+}, and Cl^{-} ions and dimethyl sulfoxide and N-(2-phenylethyl) methanesulfonamide molecules were removed. In the next stage, the lost atoms were repaired in the amino acids. After identifying the polar hydrogens, Kollman charges were added and the receptors were prepared in the purified form. Another treatment prior to molecular docking was the design of grid parameters. At this stage, after the ligand molecule was randomly placed on the receptor molecule through the program, the grid-box center of the ligand/receptor model was adjusted to completely cover the ligand molecule and the spacing was set to 0.5. After the AutoGrid was built, the docking phase was started. A very wide set of docking parameters has been prepared to move the drug molecules over the entire surface of the receptors and reveal all possible active sites. For this purpose, after the receptor was set as rigid,

hybrid Lamarckian and genetic algorithm parameters were selected and the docking was run by setting the number of genetic algorithm runs as 100, the number of evals as long as status a, and population size as 300. Thus, docking was carried out suitable for examining possible non-bond interactions such as dipole-dipole, H-bond, and hydrophobic interactions. Moreover, whether the driving force was electrostatic or van der Waals, was revealed by the root mean square displacement (RMSD) results obtained as a result of docking.

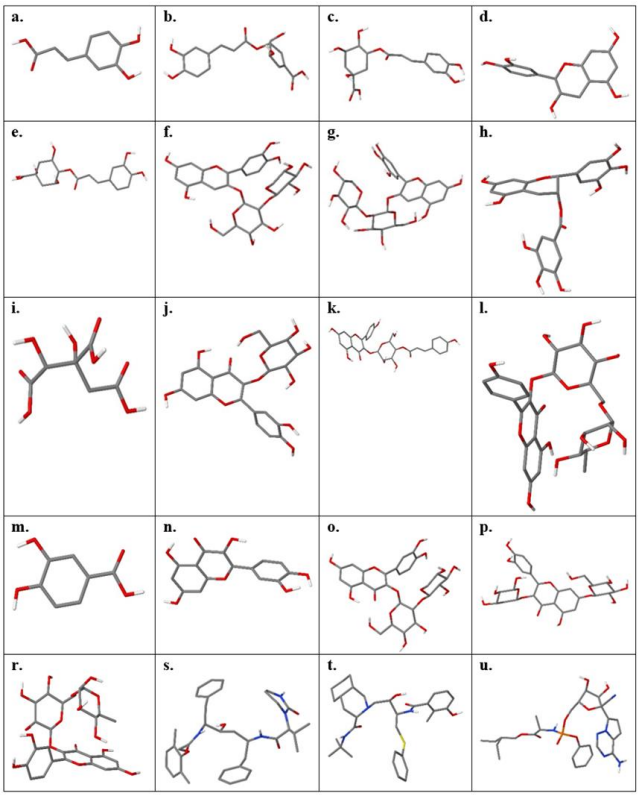

Figure 1. The structures of the ligand molecules shown in stick models. The ligands are caffeic acid (a), caffeoylshikimic acid (b), chlorogenic acid (c), cianidanol (d), cryptochlorogenic acid (e), cyanidin-3-O-beta-D-sambubioside (f), delphinidin-3-sambubioside (g), epigallocatechin gallate (h), hydroxycitric acid (i), isoquercitrin (j), kaempferol (k), nicotiflorin (l), protocatechuic acid (m), quercetin (n), quercetin-3-sambubioside (o), quercetin pentosylhexoside (p), rutin (r), lopinavir (s), nelfinavir (t), and remdesivir (u). The colors gray, red, white, blue, yellow and orange represent the elements of carbon (C), oxygen (O), hydrogen (H), nitrogen (N), sulfur (S) and phosphorus (P), respectively

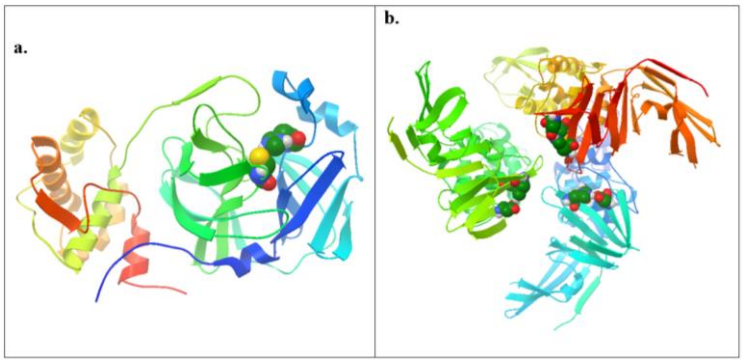

Figure 2. The secondary structures of $3CL^{pro}$ (a) and PL^{pro} (b) displayed in rainbow style with their highlighted catalytic dyad and triad amino acids as space filling model (CPK style). $3CL^{pro}$ is a single chain protease, while PL^{pro} is a bulkier molecule consisting of A, B and C chains

The free binding energy (BE) calculation was carried out as follows in Equation 1.

Estimated Free Energy of Binding = (1) + (2) + (3) - (4) (1)

(1): Final Intermolecular Energy = [vdW + Hbond + desolvation Energy] + Electrostatic Energy; (2): Final Total Internal Energy; (3): Torsional Free Energy; (4): Represents Unbound System's Energy = [(2) Final Total Internal Energy].

RESULTS AND DISCUSSION

In the fight against COVID-19, the first strategy was to test existing broad-spectrum anti-viral medications. The second strategy, on the other hand, is using databases to screen molecules for potential anti-coronavirus activity. Molecular docking studies are widely employed in drug design to better understand the interactions between a receptor and a ligand and the possible bonds between them. The number of drug-protein interactions as well as the binding energy score may be used to compare the affinity of various compounds to the specific receptor. Compounds with the lowest (most negative) score and a suitable hydrogen bond arrangement may be selected as future therapeutic targets (Steklac et al., 2021). In the meantime, the inhibition constant is useful for making predictions about the necessary dose of the drug.

In this study, two highly important proteases of CoV, PL^{pro} and $3CL^{pro}$ were targeted to find the possible interactions with the major phytochemicals of *H. sabdariffa* L., which is also known as red sorrel or roselle. 17 compounds were selected for this study that had been reported in the literature as the most abundant biomolecules of *H. sabdariffa,* including many organic acids as well as catechin and quercetin derivatives (Izquierdo-Vega et al., 2020) . Within these molecules, delphinidin-3-sambubioside ($C_{26}H_{29}O_{16}^{+}$, MW: 597.5) and cyanidin-3-O-beta-D-sambubioside ($C_{26}H_{29}ClO_{15}$, MW: 616.9) are anthocyanins. Caffeic acid ($C_9H_8O_4$, MW: 180.16) is a hydroxycinnamic acid derivative, a member of catechols. Caffeoylshikimic acid ($C_{16}H_{15}O_8^{-}$ MW: 335.28) is a hydroxy monocarboxylic acid anion. Chlorogenic acid ($C_{16}H_{18}O_9$, MW: 354.31) is a polyphenol and the ester of caffeic acid and quinic acid. Cianidanol (catechin $C_{15}H_{14}O_6$, MW: 290.27) is a polyphenol. Protocatechuic acid (3,4-dihydroxybenzoic acid) ($C_7H_6O_4$, MW: 154.12) is a member of catechols and a dihydroxybenzoic acid. Cryptochlorogenic acid ($C_{16}H_{18}O_9$, MW: 354.31) is a cinnamate ester obtained by condensation of trans-caffeic acid with quinic acid. Epigallocatechin gallate ($C_{22}H_{18}O_{11}$, MW: 458.4) is tea catechin. Hydroxycitric acid ($C_6H_8O_8$, MW: 208.12) is a citric acid derivative. Isoquercitrin ($C_{21}H_{20}O_{12}$, MW: 464.4) is a conjugate acid of a quercetin 3-O-beta-D-glucopyranoside. Kaempferol ($C_{15}H_{10}O_6$, MW: 286.24), is a tetrahydroxyflavone. Nicotiflorin ($C_{27}H_{30}O_{15}$, MW: 594.5) is a rutinoside, a trihydroxyflavone, and a kaempferol O-glucoside. Quercetin ($C_{15}H_{10}O_7$, MW: 302.23) is a pentahydroxyflavone. The structures of quercetin-3-sambubioside, and quercetin pentosylhexoside ($C_{26}H_{28}O_{16}$, MW: 596.5) are highly close to each other. Rutin ($C_{27}H_{30}O_{16}$, MW: 610.5) also a derivative of quercetin, a tetrahydroxyflavone. Great differences in the molecular weights and structures of the phytochemicals of *H. sabdariffa* were observed. Also, many compounds are quercetin derivatives, with the same number of torsions and aromatic rings. As a result, this work demonstrates the consequences of even minor structural variations in ligands on their interaction with SARS-CoV-2 receptors.

All the phytochemicals of *H. sabdariffa* used in this study were demonstrated to have a negative binding affinity against $3CL^{pro}$ and PL^{pro}, which were graded accordingly to belong to the model with the lowest energy. These are shown in Table 1 and Table 2, respectively. On the other hand, lopinavir, nelfinavir and remdesivir, were used as the positive controls, which are Food and Drug Administration (FDA)-approved drugs. SARS-CoV-2 replication has been reported to be inhibited by nelfinavir (Ohashi et al., 2021). Nelfinavir was also shown to interact with the main protease of COVID-19 with a -7.30 kcal/mol binding energy (Arif, 2022). Lopinavir, on the other hand, has been generally used in combination with ritonavir. However, lopinavir is not recommended any more by the World Health Organization (WHO) as a SARS-CoV-2 medication (Cattaneo et al., 2020). Another study reported that lopinavir does not possibly interact with the major targets like $3CL^{pro}$ and PL^{pro} (Wu et al., 2020).

In our study, no H-bond interactions between lopinavir and the 3CLpro and PL^{pro} receptors were detected. Currently, only remdesivir is recommended by WHO as the SARS-CoV-2 medication (WHO, 2022). Remdesivir has been developed in response to the Ebola outbreak in West Africa from 2014 to 2016. Remdesivir has also been reported to have activity against a wide range of ssRNA viruses (Ghanbari et al., 2020). This study verifies the good interaction of remdesivir with $3CL^{pro}$ and PL^{pro}.

$3CL^{pro}$/ligands docking analysis

Compounds with a binding affinity of −6.5 kcal/mol or less are assumed to be better inhibitors of SARS CoV-2 (Table 1). Low binding energies of the compounds of caffeoylshikimic acid (-7.72 kcal/mol), chlorogenic acid (-7.18 kcal/mol), cianidanol (-7.10 kcal/mol), cryptochlorogenic acid (-6.67 kcal/mol), and kaempferol (-6.82 kcal/mol) were calculated to $3CL^{pro}$. The other compounds with more than -6.50 binding energies to $3CL^{pro}$ were found to be caffeic acid, cyanidin-3-O-beta-D-sambubioside, delphinidin-3-sambubioside, epigallocatechin gallate, hydroxycitric acid, isoquercitrin, nicotiflorin, protocatechuic acid, quercetin, quercetin-3-sambubioside, quercetin pentosylhexoside, and rutin. In the meantime, the interactions of antiviral drugs with $3CL^{pro}$ were also studied. As expected, low binding energies of lopinavir (-6.74 kcal/mol), nelfinavir (-10.16 kcal/mol), and remdesivir (-6.40 kcal/mol) were obtained for $3CL^{pro}$. In this study, no compounds have been shown to possess better affinity than nelfinavir, which was found to have the lowest binding energy (-10.16 kcal/mol) to $3CL^{pro}$. Caffeoylshikimic acid, chlorogenic acid, cianidanol, and kaempferol, on the other hand, had a higher binding affinity to $3CL^{pro}$ than lopinavir and remdesivir.

Table 1. The binding energies, inhibition constants and H-bonds between the ligands and $3CL^{pro}$ protein

Ligand molecules	Model	BE (kcal/mol)	IC (µM)	Detected H-bonds (Å)
caffeic acid	88	-5.77	59.13	VAL303(1.790,1.938) GLN299(2.236) MET6(2.028)
caffeoylshikimic acid	52	-7.72	2.20	ASN142(1.84, 2.097) THR190(1.875, 1.985) GLN192(1.905) GLU166(2.049) HIS163(1.884)
chlorogenic acid	8	-7.18	5.45	ASN142(1.684, 2.039) THR190(1.703, 1.923) HIS163(2.073) GLN192(1.771)
cianidanol	88	-7.10	6.29	MET6(2.001) ASP295(2.028) VAL303(2.049) THR304(2.0, 2.101)
cryptochlorogenic acid	34	-6.67	12.96	GLN192(1.685) GLN189(2.082) THR190(2.122) CYS44(2.056)
cyanidin-3-O-beta-D-sambubioside	9	-4.28	725.07	LYS137(1.937) GLN127(1.757, 2.157, 2.212) VAL125(1.98, 2.092) SER123(1.951) SER139(1.767)
delphinidin-3-sambubioside	70	-5.00	216.12	CYS44(2.029) ASN142(2.042, 2.127) ARG188(1.942)
epigallocatechin gallate	6	-6.40	20.41	THR190(1.839, 1.877) GLN192(2.055) GLU166(1.883) LEU141&SER144(2.016)

Table 1. The binding energies, inhibition constants and H-bonds between the ligands and 3CL^{pro} protein (Continued)

hydroxycitric acid	70	-4.19	855.65	THR280(2.162) GLY283(1.803)
isoquercitrin	94	-5.76	60.03	GLN83(1.754, 1.835) GLU178(1.873, 2.044) LYS88(1.894, 2.216) TYR101(1.887)
kaempferol	56	-6.82	10.08	LYS12(2.15) ASP33(2.024) PRO96(2.006) THR98(2.083)
nicotiflorin	90	-5.38	113.27	ASN142(2.248) GLY143(2.086) GLU166(2.102) GLN189(2.127)
protocatechuic acid	58	-5.03	204.15	GLU166(1.94) GLN192(1.752) THR190(1.754, 1.833, 2.154)
quercetin	1	-6.14	31.57	MET6(2.04)
quercetin-3-sambubioside	34	-5.05	200.16	LEU141(1.899) GLU166(1.743, 2.105) GLN189(1.888)
quercetin pentosylhexoside	68	-6.48	17.65	TYR154(2.248, 2.249)
rutin	43	-5.28	134.99	GLN189(1.933, 2.067, 2.246) HIS163(2.183) ASN142(2.16) PHE140(2.04)
lopinavir	85	-6.74	11.43	-
nelfinavir	49	-10.16	0.04	GLN299(1.991) VAL303(1.878, 1.999)
remdesivir	87	-6.40	20.20	SER46(1.939) HIS164(2.079) GLU166(1.779)

The hydrogen bond is an intermolecular force that keeps two or more molecules together and is required for the stability of protein-ligand interactions (Gouhar et al., 2021). As shown in Table 1, the caffeoylshikimic acid/3CL^{pro} complex model 52 revealed seven H-bonds with the lowest binding energy (-7.72 kcal/mol). Chlorogenic acid/3CL^{pro} complex, which has the second lowest binding energy, was found to form six H-bonds. Cianidanol/3CL^{pro} and kaempferol/3CL^{pro} complexes exhibited 5 H-bonds and 4 H-bonds, respectively. However, the hydroxycitric acid/3CL^{pro} model with the highest binding energy (-4.19 kcal/mol) was observed to reveal two H-bonds. One bond was with THR280 at a distance of 2.162 Å and the other with GLY283 at 1.803 Å. A variable number of H-bond interactions between quercetin and its derivatives with 3CL^{pro} were recorded. Also, the binding energies were shown to be moderately different. In the meantime, numerous studies have found quercetin and its various derivatives to have strong binding affinities with 3CL^{pro}. In particular, the importance of hydroxyl groups was highlighted for the occurrence of H-bond interactions (Mouffouk et al., 2021). Furthermore, quercetin, one of the most important plant molecules, was reported to interact with the S protein–human ACE2 receptor interface, thereby, being found to be capable of interfering with SARS-CoV-2 replication. The pharmacological activities of quercetin include antiviral, anti-atopic, pro-metabolic, and anti-inflammatory effects (Derosa et al., 2021). Therefore, quercetin and its derivatives could be good candidates to fight against COVID-19.

Another issue that draws attention in Table 1 is the results of the anti-viral drugs that make up the last 3 rows. According to these results, the binding affinity of nelfinavir was determined to be the highest of all to the 3CL^{pro} receptor. As a matter of fact, the energy of the model numbered 49 was recorded as the lowest, at -10.16 kcal/mol. Nelfinavir was also discovered to generate three H-bonds with 3CL^{pro}. These are produced between the H atom of the ligand and the O atom of the receptor

(around 2 Å). The binding energy of the remdesivir/3CL^{pro} complex with 87 as the model number was found to be -6.40 kcal/mol. In this model, three H-bonds were seen at around 2 Å. Two H bonds were detected between the H atom of the ligand and the O atom of the receptor. The other H bond was occurred between the O atom of the ligand and the H atom of the receptor. In a recent study, the interaction of remdesivir and the 3CL^{pro} complex was reported to have a -8.2 kcal/mol binding energy with many H-bonds (Naik et al., 2021). Interestingly, no bond formation was followed-up in the lopinavir/3CL^{pro} complex in which a -6.74 kcal/mol binding free energy was shown at model number 85. However, hydrophobic interactions of the lopinavir/3CL^{pro} complex were observed at the amino acids of MET49, MET165, and LEU141.

Considering all these results, it can be pronounced that the interactions are increased and become more frequent at GLN192, GLN189, THR190, GLU166, HIS163, LEU141, and SER144 amino acids in the ligand/3CL^{pro} receptor complexes. These residues are not in the catalytic dyad, but highly close to this area of 3CL^{pro}. Thus, it may be concluded that the ligands investigated in this work, particularly caffeoylshikimic acid and chlorogenic acid, interact with 3CL^{pro} in a location closer to the catalytic dyad.

Another remarkable column in Table 1 belongs to the inhibition constant (IC). The more negative binding energy and smaller value of IC imply a best docking score (Singh et al., 2022). The most striking finding in Table 1 is that the inhibition constant values decrease as the binding energies fall. For example, the lowest binding energy belongs to the nelfinavir/3CL^{pro} model (-10.16 kcal/mol), which has a 0.04 µM IC value. On the other hand, the IC value of remdesivir/3CL^{pro} (-6.40 kcal/mol) was calculated to be 20.20 µM. The IC values of caffeoylshikimic acid, chlorogenic acid, cianidanol, and kaempferol were computed to be 2.20, 5.45, 6.29, and 10.08 µM, respectively. Therefore, the abovementioned molecules were shown to have low binding energies with low IC values, leading to high binding affinities to 3CL^{pro}. On the contrary, the highest binding energy was found to be -4.19 kcal/mol belonging to the hydroxycitric acid/3CL^{pro} model, which has an 855.65 µM IC value, leading to a low binding affinity. This trend was also followed for all models. Additionally, the decreasing inhibition state was observed throughout the 100-step docking of all models, in contrast to the increasing interaction state.

PL^{pro}/ligands docking analysis

The molecular docking revealed that among the 17 chemical compounds tested, 7 of them possess a low binding energy (-6.50 kcal/mol or less) and therefore have a good interaction with PL^{pro} (Table 2). The compounds of caffeoylshikimic acid (-6.73 kcal/mol), chlorogenic acid (-7.20 kcal/mol), cianidanol (-6.85 kcal/mol), delphinidin-3-sambubioside (-6.66 kcal/mol), kaempferol (-7.07 kcal/mol), nicotiflorin (-7.40 kcal/mol), and quercetin pentosylhexoside (-6.54 kcal/mol) owned the binding energies of -6.50 kcal/mol and less with PL^{pro}. Nicotiflorin was shown to have the lowest binding energy (-7.40 kcal/mol). On the other hand, the binding energies between lopinavir (-8.33 kcal/mol), nelfinavir (-9.10 kcal/mol) and remdesivir (-7.80 kcal/mol) with PL^{pro} have been demonstrated to be lower than any other ligand.

Table 2. The binding energies, inhibition constants and H-bonds between the ligands and PL^{pro} protein

Ligand molecules	Model	BE (kcal/mol)	IC (µM)	Detected H-bonds (Å)
caffeic acid	85	-5.77	59.38	THR74C(1.774) LEU80C(1.812)
caffeoylshikimic acid	60	-6.73	11.76	TYR251B(1.975) LYS217B(2.026) LYS306B(1.852,1.915)
chlorogenic acid	53	-7.20	5.24	ASP76A(2.004) LEU80A(2.029) ARG65A(1.841) LYS43B(1.939)
cianidanol	72	-6.85	9.49	THR74B(1.945) LEU80B(2.032)
cryptochlorogenic acid	5	-6.04	37.49	THR75B(1.858) PRO77B(2.019) LEU80B(2.001) LYS45C(2.105)
cyanidin-3-O-beta-D-sambubioside	7	-5.12	177.57	GLU161A&THR158A(2.047) GLN269C(1.764) ASN109C(2.084,2.093) LEU162C(2.09)
delphinidin-3-sambubioside	17	-6.66	13.24	GLY163B(1.823) GLU167B(1.959, 2.197) LYS157B(2.036) ASP108C(1.890, 2.138)
epigallocatechin gallate	93	-5.95	43.42	LYS217B(2.075, 2.112) THR257B(1.986) LYS306B(2.196) GLY256B(1.962) GLU307B(1.841, 1.842) ASN308B(1.174)
hydroxycitric acid	70	-3.63	2170.00	THR257B(2.023) LYS254B(2.183) TYR251B(1.83) GLU214B(1.915) TYR305B(1.972, 1.994)
isoquercitrin	2	-6.31	23.80	LYS43A(1.915, 1.952) ARG65C(1.929) THR75C(2.244) LEU80C(2.054)
kaempferol	68	-7.07	6.53	THR158A(1.824) ASP108B(1.903) LYS157B(2.25) LEU162B(1.978) ASN109C(2.121)
nicotiflorin	80	-7.40	3.75	LYS43C(1.766)
protocatechuic acid	32	-5.42	105.86	THR74C(1.846) LEU80C(1.688)
quercetin	88	-6.25	26.11	THR74B(2.01) LEU80B(2.03) LYS43C(2.139, 2.141)
quercetin-3-sambubioside	63	-5.36	118.50	ASP108B(1.89) ASN109C(1.678)
quercetin pentosylhexoside	53	-6.54	16.06	LYS92A(1.877, 1.997) LYS105A(1.571) TRP106A(1.927) ASP108A(1.806, 2.171) ASP286A(1.897, 2.011) ALA288A(2.058)
rutin	75	-5.85	51.85	GLN195A(2.061, 2.173) GLN196A(1.865, 1.870, 2.143) CYS192A(1.926, 2.243)
lopinavir	25	-8.33	0.79	-
nelfinavir	4	-9.10	0.21	LEU162B(1.932)
remdesivir	48	-7.80	1.90	THR75A(1.78) LYS45B(2.144)

The H-bonds in the ligand-receptor complex explain more about the binding affinity. In this regard, the nicotiflorin/PL^{pro} complex, which unveiled the lowest binding energy at a model number of 80, was found to form only 1 H-bond with 1.766 Å. Chlorogenic acid/PL^{pro} complex, which has shown the second lowest binding energy at a model number of 53, was found to form four H-bonds. On the other hand, epigallocatechin gallate/PL^{pro} with model number 93, which was shown to have a -5.95 kcal/mol binding energy, was found to possess 8 H-bond interactions. In the meantime, the quercetin pentosylhexoside/PL^{pro} complex with model number 53 was depicted to have low binding energy (-6.54 kcal/mol) with 9 H-bonds, which stands as the highest number of H-bonds in all complexes. Clearly, the H-bond interactions of our ligands, especially quercetin pentosylhexoside with PL^{pro}, suggest a high binding affinity. Interestingly, H-bond formations between the antiviral drugs and the PL^{pro} receptor complex were detected to be low in number. This fact was followed throughout the docking procedures for all 100 conformations. For example, the nelfinavir/ PL^{pro} complex with the lowest binding energy (-9.10 kcal/mol) was found to have only 1 H-bond with a distance of around 2 Å. This H bond occurred between the O atom belonging to the aromatic –OH of the ligand and the H atom of the receptor. On the other hand, two H-bonds consisted of remdesivir/PL^{pro} complex. One of the H bonds was found between the H atom of the ligand and the O atom of THR75A. The other H bond was seen between the H atom of LYS45B and the O atom of the remdesivir. In the lopinavir/ PL^{pro} complex, no H-bond formation appeared, however, hydrophobic interactions at GLY160A, LEU162A, VAL159B, GLY160B, LEU162B, GLY160C, and LEU162C amino acids in which different types of chains were monitored. Another important result in Table 2 is that the H-bond interactions increase and become more frequent in the regions of LYS43B and LYS43C, LEU80B, LEU80C, and LEU162B amino acids of the PL^{pro} receptor for all ligand molecules. Accordingly, it can be suggested that the most favorable polypeptide chains are B and C chains. On the other hand, IC values decreased, in contrast to increasing interaction as in the previous model. For example, the IC value of 0.21 μM for the nelfinavir/PL^{pro} model was calculated as 2170 μM for the hydroxycitric acid/PL^{pro} model, which has the lowest interaction. The IC value of nicotiflorin, on the other hand, was determined to be 3.75 μM which is the closest value to the one with remdesivir. Also, our ligands with low binding energies revealed low IC values such as chlorogenic acid (5.24 μM) and kaempferol (6.53 μM), suggesting high binding affinities.

For a better understanding of the data in Tables 1 and 2, the interactions of the most favorable *H. sabdariffa* components in both ligand/receptor models and those of antiviral drugs are illustrated in Figures 3 and 4. It is clear from Figure 3 that strong interactions between caffeoylshikimic acid, chlorogenic acid, cianidanol, cryptochlorogenic acid, epigallocatechin gallate, kaempferol, and quercetin pentosylhexoside with $3CL^{pro}$ were monitored. Also, good interactions of nelfinavir and remdesivir (Figure 3i and Figure 3j) which have been already proven to be anti SARS-CoV-2 medications, were determined. However, the illustration of the lopinavir/$3CL^{pro}$ complex evidently shows no H-bond formations as seen in Figure 3h.

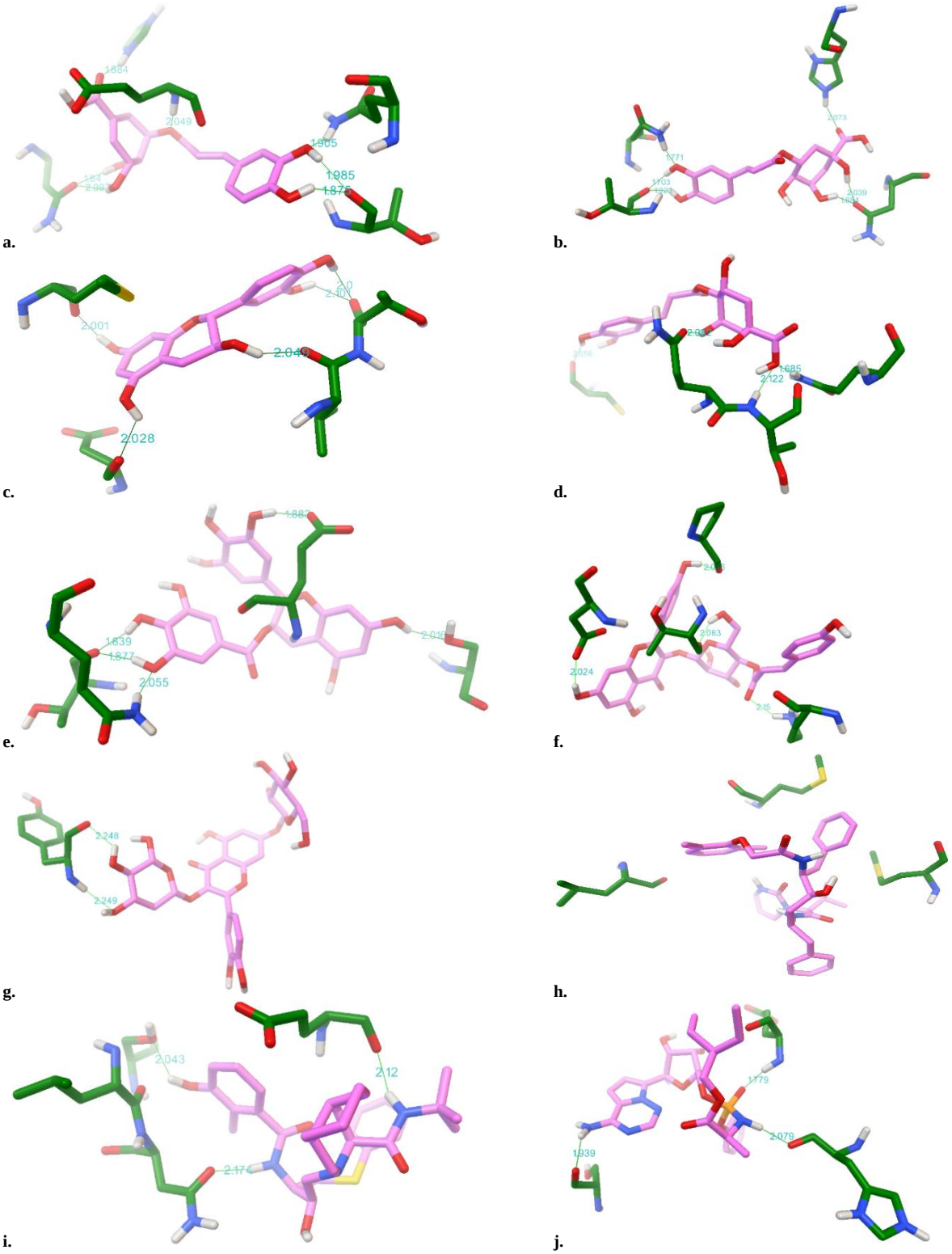

Figure 3. The interactions of ligands/3CL^{pro} models. The ligands are caffeoylshikimic acid (a), chlorogenic acid (b), cianidanol (c), cryptochlorogenic acid (d), epigallocatechin gallate (e), kaempferol (f), quercetin pentosylhexoside (g), lopinavir (h), nelfinavir (i), remdesivir (j)

Figure 4a-4g illustrates the interactions of caffeoylshikimic acid, chlorogenic acid, cianidanol, delphinidin-3-sambubioside, kaempferol, nicotiflorin, and quercetin pentosylhexoside with PL^{pro}. Strong interactions of the abovementioned molecules with PL^{pro} were revealed. Additionally, nelfinavir/PL^{pro} and remdesivir/PL^{pro} revealed strong H-bond interactions, however, like in the previous illustration, lopinavir/PL^{pro} interaction was observed to be weak, as seen in Figure 4h.

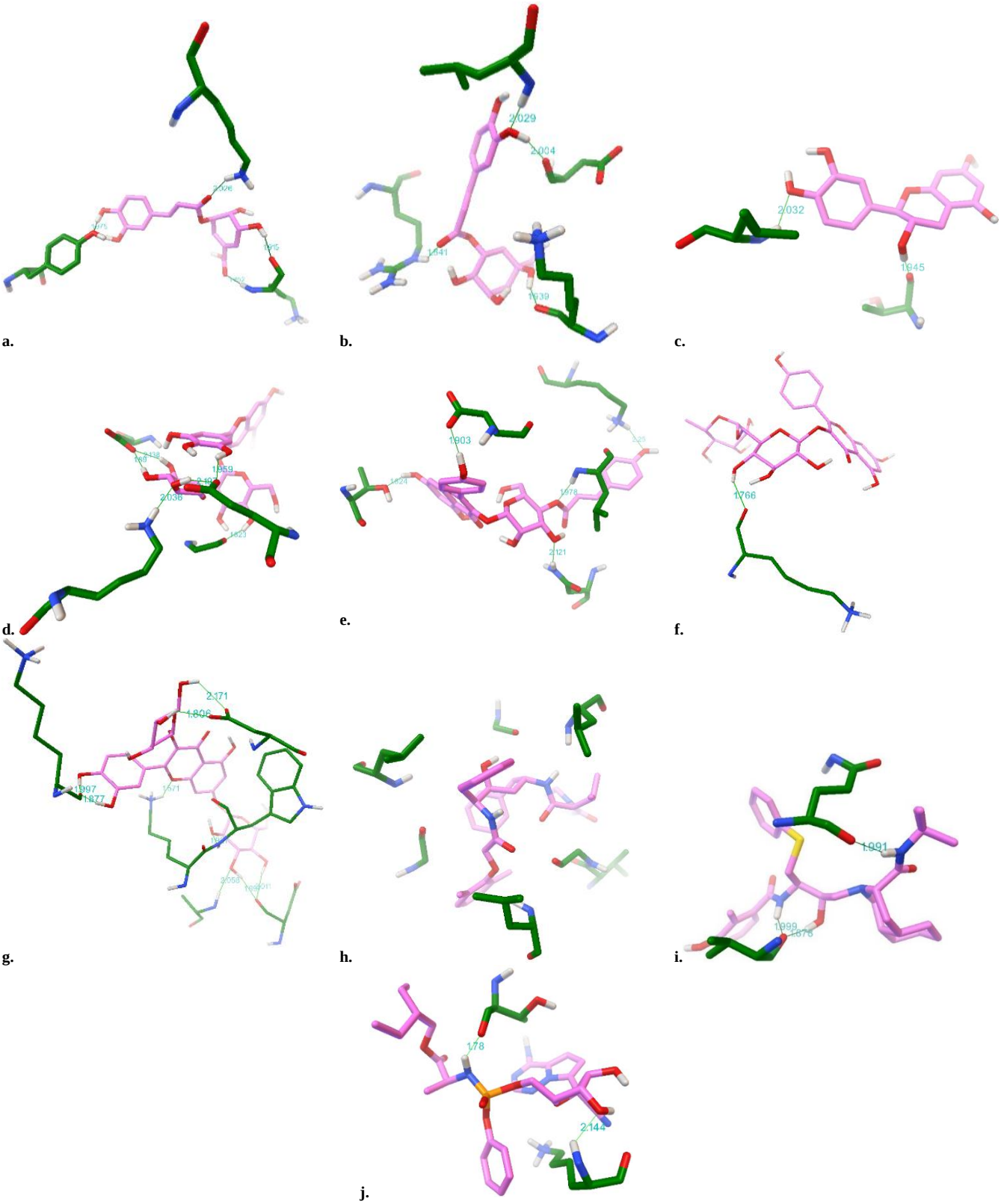

Figure 4. The interactions of ligands/PL^{pro} models. The ligands are caffeoylshikimic acid (a), chlorogenic acid (b), cianidanol (c), delphinidin-3-sambubioside (d), kaempferol (e), nicotiflorin (f), quercetin pentosylhexoside (g), lopinavir (h), nelfinavir (i), remdesivir (j)

Looking at all the docking models, it was noted that the driving force of the interaction was non-bond interactions. In this regard, van der Waals interactions were monitored to be the most contributing interactions, however, the electrostatic interactions remained at minimal levels. For example, in the nelfinavir/3CL^{pro} complex, van der Waals interactions were found to be -13.57 kcal/mol, while electrostatic interaction was shown to be -0.17 kcal/mol. Similarly, in the

nelfinavir/PL^{pro} complex, van der Waals and electrostatic interactions were calculated to be -12.55 kcal/mol, and -0.13 kcal/mol, respectively.

The interaction energies of the ligands/receptors were not detected in parallel with the molecular weight. For example, the binding energy of rutin/3CL^{pro}, which is the bulkiest ligand of all, was found to be -5.28 kcal/mol, while it was found to be -5.03 kcal/mol for the smallest ligand, protocatechuic acid. This phenomenon is also correct for ligands/PL^{pro} receptor complexes. In the meantime, the interaction energies of quercetin-3-sambubioside and quercetin pentosylhexoside, the ligands highly similar in structure, were found to be moderately different with both receptors. Also, the former has been shown to have 2 H-bonds with PL^{pro}, while the latter has 9 H-bonds. Therefore, even a small difference in the structure changed the interaction tremendously.

Rutin (quercetin-3-O-rutinoside**)** was already co-crystallized with 3CL^{pro} (Shawky et al., 2020). In our study, the binding energy of rutin/3CL^{pro} with model number 43 was computed to be -5.28 kcal/mol. A strong interaction between rutin and 3CL^{pro} was demonstrated with 7 H-bonds with 134.99 µM as the inhibition constant. In the meantime, the rutin/PL^{pro} complex owned a binding energy of -5.85 kcal/mol with 3 H-bonds, and a 51.85 µM IC value. Strong interactions of rutin with both receptors were shown, as illustrated in Figure 5. Although the IC values of both complexes are relatively high, the high number of H-bonds could result in a strong interaction between rutin and the proteases. These results highlight the importance of H-bonds in ligand/receptor complexes. Also, it is clear from Figure 1r and Figure 1l that rutin and nicotiflorin have a structural similarity with the same molecular formula. Additionally, the binding energies and H-bonds of the nicotiflorin/3CL^{pro} and rutin/3CL^{pro} models were found to be highly close (Table 1). Therefore, a strong interaction between nicotiflorin and 3C-pro can be proposed. In the meantime, the moderately low binding energy of nicotiflorin/PL^{pro} was determined with only 1 H-bond and a low IC value (3.75 µM). However, the rutin/PL^{pro} model was seen to have a high binding energy as compared to the previous model, with 7 H-bonds and an IC value of 51.85 µM. In this regard, nicotiflorin possesses a high binding affinity for PL^{pro}, suggesting a better candidate to inhibit PL^{pro} activity.

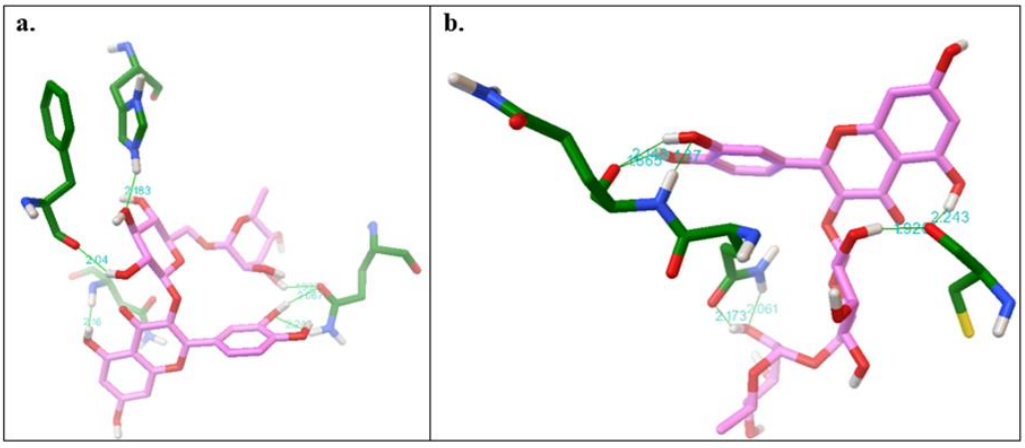

Figure 5. The H-bond interactions of rutin/3CL^{pro} (a), and rutin/PL^{pro} (b) models

Recently, several plant-based compounds have been reported to possibly interact with coronavirus receptors. From these studies (+)-lariciresinol 9′-p-coumarate (-15.12 kcal/mol), β-sitosterol acetate (-14.14 kcal/mol), sesquipinsapol B(-13.39 kcal/mol), and campesterol (-13.25 kcal/mol) which are the compounds of softwood bark were reported to exhibit excellent docking scores with the receptor 3CL^{pro} (Jablonsky et al., 2022). In another study, the phytochemicals of broussoflavan A (-91.22 kcal/mol), dieckol (-73.11 kcal/mol), hygromycin B (-62.48

kcal/mol), sinigrin (-65.08 kcal/mol), and theaflavin-3,3′-digallate (-76.85 kcal/mol) were reported to exhibit excellent SARS-CoV-2 $3CL^{pro}$ inhibitors (Al-Sehemi et al., 2022). The binding affinities of the abovementioned compounds with $3CL^{pro}$ were found to be better than the compounds studied in this research. Furthermore, ribavirin (PDB code: 3e9s) was reported to have very low binding energy (-38.58 kcal/mol) with PL^{pro}. Many H-bonds were reported in the complex, suggesting a strong interaction between ribavirin and PL^{pro} (Wu et al., 2020). On the other hand, the antiviral drug zanamivir (-8.843 kcal/mol), and anti-cancer drug carfilzomib (-8.924 kcal/mol) were reported to reveal low binding energies to 3CLpro. However, adeflavin that is a medicine for B2 deficiency and coenzyme-A was shown to reveal even better docking score (-10.339 kcal/mol). Remdesivir, on the other hand, has been reported to have a -7.215 kcal/mol binding energy to $3CL^{pro}$ (Hall et al., 2020). However, in our study we have shown a binding energy of -6.40 kcal/mol between remdesivir and $3CL^{pro}$.

Previously, *H. sabdariffa* bioactive compounds were recommended to block coronavirus binding (Parga-Lozano, 2020). *Hibiscus noldeae*, another species traditionally used for respiratory diseases, was recently reported to be fractioned and some of the bioactive compounds were isolated. The fractions and isolated compounds (caffeic acid and isoquercetin) of *H. noldeae* were shown to possess anti-inflammatory activities. These compounds and the fractions were reported to have significant inhibitory effects on caspase-1 activities, and on IL-1β and IL-6 production (Tomani et al., 2020). Some of the compounds of *Hibiscus* have been illustrated so far to interact with CoV. Delphinidin 3-O, (6′′-O-malonyl)-beta-D-glucoside-3′-O-beta-D-glucoside (-11.624), cyanidin-3,5-diglucoside (-9.754), and delphinidin-3-sambubioside (-11.061) from *H. sabdariffa* was reported to have interactions with $3CL^{pro}$. In our study, a -6.66 kcal/mol binding energy of delphinidin-3-sambubioside/PL^{pro} complex with six H-bonding interactions were determined. Also, a -5.00 kcal/mol binding energy of delphinidin-3-sambubioside/$3CL^{pro}$ complex with four H-bond formations were detected. Furthermore, gallocatechin galllate and epigallocatechin gallate were shown to interact with $3CL^{pro}$ of which galloyl moiety was found to be important for the binding to the $3CL^{pro}$ active site pocket (Nguyen et al., 2012). Our study is in parallel to the aforementioned study, with the demonstration of the low binding energy of epigallocatechin gallate/$3CL^{pro}$ and many H-bond interactions. Additionally, synthetic catechin derivatives were reported to interact with $3CL^{pro}$ (PDB ID: 6LU7) with a -8.0 kcal/mol binding energy as the lowest value (Arif, 2022).

CONCLUSION

In this study, we investigated the interactions of 17 major compounds of *H. sabdariffa* with $3CL^{pro}$ and PL^{pro}, the main proteases of SARS-CoV-2. For the targets of both $3CL^{pro}$ and PL^{pro}, caffeoylshikimic acid, chlorogenic acid, cianidanol, and kaempferol have been demonstrated to possess binding affinities of −6.5 or less. The lowest binding energies and the presence of H-bond interactions in our ligands of caffeoylshikimic acid, chlorogenic acid, and cianidanol with the $3CL^{pro}$ complex indicate the existence of strong interactions between these 3 natural compounds and our target protein. For the ligands/ PL^{pro} complexes, chlorogenic acid, delphinidin-3-sambubioside and quercetin pentosylhexoside with the PL^{pro} complex exhibited the lowest binding energies and higher H-bond interactions. It was observed that the driving force of both ligand/receptor models was non-bond interactions, and the greatest contribution was aroused by van der Waals interactions. On the other hand, electrostatic interactions remained minimal at the zero level. This study demonstrates that many phytochemicals of *H. sabdariffa* could possibly interact with the main proteases of SARS-CoV-

2, namely $3CL^{pro}$ and PL^{pro}. Therefore, this study suggests that most of these phytochemicals inhibit the activities of $3CL^{pro}$ and PL^{pro}.

ACKNOWLEDGEMENTS

Computing resources for Molecular Docking studies calculations reported in this paper were fully performed at Harran University High Performance Computing Center (Harran HPC resources).

Conflict of Interest

The article authors declare that there is no conflict of interest between them.

Author's Contributions

The authors declare that they have contributed equally to the article.

REFERENCES

Agrawal N, Goyal A, 2022. Potential Candidates against COVID-19 Targeting RNA-Dependent RNA Polymerase: A Comprehensive Review. Current pharmaceutical biotechnology, 23(3): 396-419.

Al-Sehemi AG, Pannipara M, Parulekar RS, Kilbile JT, Choudhari PB, Shaikh MH, 2022. In silico exploration of binding potentials of anti SARS-CoV-1 phytochemicals against main protease of SARS-CoV-2. Journal of Saudi Chemical Society, 26(3): 101453.

Amin SA, Ghosh K, Singh S, Qureshi IA, Jha T, Gayen S, 2022. Exploring naphthyl derivatives as SARS-CoV papain-like protease (PLpro) inhibitors and its implications in COVID-19 drug discovery. Molecular diversity, 26(1): 215-228.

Arif MN, 2022. Catechin Derivatives as Inhibitor of COVID-19 Main Protease (Mpro): Molecular Docking Studies Unveil an Opportunity Against CORONA. Combinatorial chemistry & high throughput screening, 25(1): 197-203.

Cattaneo D, Cattaneo D, Gervasoni C, Corbellino M, Galli M, Riva A, Gervasoni C, Clementi E, Clementi E, 2020. Does lopinavir really inhibit SARS-CoV-2? Pharmacological research, 158: 104898.

Chen CC, Yu X, Kuo CJ, Min J, Chen S, Ma L, Liu K, Guo RT, 2021. Overview of antiviral drug candidates targeting coronaviral 3C-like main proteases. The FEBS journal, 288(17): 5089-5121.

Da-Costa-Rocha I, Bonnlaender B, Sievers H, Pischel I, Heinrich M, 2014. Hibiscus sabdariffa L. - a phytochemical and pharmacological review. Food chemistry, 165: 424-443.

Deb SD, Jha RK, Jha K, Tripathi PS, 2022. A multi model ensemble based deep convolution neural network structure for detection of COVID19. Biomedical signal processing and control, 71: 103126.

Derosa G, Maffioli P, D'Angelo A, Di Pierro F, 2021. A role for quercetin in coronavirus disease 2019 (COVID-19). Phytotherapy research : PTR, 35(3): 1230-1236.

Dong W, Wei X, Zhang F, Hao J, Huang F, Zhang C, Liang W, 2014. A dual character of flavonoids in influenza A virus replication and spread through modulating cell-autonomous immunity by MAPK signaling pathways. Scientific reports, 4: 7237.

Douangamath A, Fearon D, Gehrtz P, Krojer T, Lukacik P, Owen CD, Resnick E, Strain-Damerell C, Aimon A, Abranyi-Balogh P, Brandao-Neto J, Carbery A, Davison G, Dias A, Downes TD, Dunnett L, Fairhead M, Firth JD, Jones SP, Keeley A, Keseru GM, Klein HF, Martin MP, Noble MEM, O'Brien P, Powell A, Reddi RN, Skyner R, Snee M, Waring MJ, Wild C, London N, von Delft F, Walsh MA, 2020. Crystallographic and electrophilic fragment screening of the SARS-CoV-2 main protease. Nature communications, 11(1): 5047.

Ghanbari R, Teimoori A, Sadeghi A, Mohamadkhani A, Rezasoltani S, Asadi E, Jouyban A, Sumner SC, 2020. Existing antiviral options against SARS-CoV-2 replication in COVID-19 patients. Future microbiology, 15: 1747-1758.

Ghosh AK, Raghavaiah J, Shahabi D, Yadav M, Anson BJ, Lendy EK, Hattori SI, Higashi-Kuwata N, Mitsuya H, Mesecar AD, 2021. Indole Chloropyridinyl Ester-Derived SARS-CoV-2 3CLpro Inhibitors: Enzyme Inhibition, Antiviral Efficacy, Structure-Activity Relationship, and X-ray Structural Studies. Journal of medicinal chemistry, 64(19): 14702-14714.

Gouhar SA, Elshahid ZA, 2021. Molecular docking and simulation studies of synthetic protease inhibitors against COVID-19: a computational study. Journal of biomolecular structure & dynamics: 1-21.

Hall DC, Jr., Ji HF, 2020. A search for medications to treat COVID-19 via in silico molecular docking models of the SARS-CoV-2 spike glycoprotein and 3CL protease. Travel medicine and infectious disease, 35: 101646.

Hapsari BW, Manikharda, Setyaningsih W, 2021. Methodologies in the Analysis of Phenolic Compounds in Roselle (Hibiscus sabdariffa L.): Composition, Biological Activity, and Beneficial Effects on Human Health. Horticulturae, 7(2): 35.

Izquierdo-Vega JA, Arteaga-Badillo DA, Sanchez-Gutierrez M, Morales-Gonzalez JA, Vargas-Mendoza N, Gomez-Aldapa CA, Castro-Rosas J, Delgado-Olivares L, Madrigal-Bujaidar E, Madrigal-Santillan E, 2020. Organic Acids from Roselle (Hibiscus sabdariffa L.)-A Brief Review of Its Pharmacological Effects. Biomedicines, 8(5).

Jablonsky M, Steklac M, Majova V, Gall M, Matuska J, Pitonak M, Bucinsky L, 2022. Molecular docking and machine learning affinity prediction of compounds identified upon softwood bark extraction to the main protease of the SARS-CoV-2 virus. Biophysical chemistry, 288: 106854.

Kumar V, Roy K, 2020. Development of a simple, interpretable and easily transferable QSAR model for quick screening antiviral databases in search of novel 3C-like protease (3CLpro) enzyme inhibitors against SARS-CoV diseases. SAR and QSAR in environmental research, 31(7): 511-526.

McKee DL, Sternberg A, Stange U, Laufer S, Naujokat C, 2020. Candidate drugs against SARS-CoV-2 and COVID-19. Pharmacological research, 157: 104859.

Mody V, Ho J, Wills S, Mawri A, Lawson L, Ebert M, Fortin GM, Rayalam S, Taval S, 2021. Identification of 3-chymotrypsin like protease (3CLPro) inhibitors as potential anti-SARS-CoV-2 agents. Communications biology, 4(1): 93.

Morris GM, Huey R, Lindstrom W, Sanner MF, Belew RK, Goodsell DS, Olson AJ, 2009. AutoDock4 and AutoDockTools4: Automated docking with selective receptor flexibility. Journal of computational chemistry, 30(16): 2785-2791.

Mouffouk C, Mouffouk S, Mouffouk S, Hambaba L, Haba H, 2021. Flavonols as potential antiviral drugs targeting SARS-CoV-2 proteases (3CL(pro) and PL(pro)), spike protein, RNA-dependent RNA polymerase (RdRp) and angiotensin-converting enzyme II receptor (ACE2). European journal of pharmacology, 891: 173759.

Naik VR, Munikumar M, Ramakrishna U, Srujana M, Goudar G, Naresh P, Kumar BN, Hemalatha R, 2021. Remdesivir (GS-5734) as a therapeutic option of 2019-nCOV main protease - in silico approach. Journal of biomolecular structure & dynamics, 39(13): 4701-4714.

Nguyen TT, Woo HJ, Kang HK, Nguyen VD, Kim YM, Kim DW, Ahn SA, Xia Y, Kim D, 2012. Flavonoid-mediated inhibition of SARS coronavirus 3C-like protease expressed in Pichia pastoris. Biotechnology letters, 34(5): 831-838.

Nouadi B, Ezaouine A, El Messal M, Blaghen M, Bennis F, Chegdani F, 2021. Prediction of Anti-COVID 19 Therapeutic Power of Medicinal Moroccan Plants Using Molecular Docking. Bioinformatics and biology insights, 15: 11779322211009199.

Ohashi H, Watashi K, Saso W, Shionoya K, Iwanami S, Hirokawa T, Shirai T, Kanaya S, Ito Y, Kim KS, Nomura T, Suzuki T, Nishioka K, Ando S, Ejima K, Koizumi Y, Tanaka T, Aoki S, Kuramochi K, Suzuki T, Hashiguchi T, Maenaka K, Matano T, Muramatsu M, Saijo M, Aihara K, Iwami S, Takeda M, McKeating JA, Wakita T, 2021. Potential anti-COVID-19 agents, cepharanthine and nelfinavir, and their usage for combination treatment. iScience, 24(4): 102367.

Omrani M, Keshavarz M, Nejad Ebrahimi S, Mehrabi M, McGaw LJ, Ali Abdalla M, Mehrbod P, 2020. Potential Natural Products Against Respiratory Viruses: A Perspective to Develop Anti-COVID-19 Medicines. Frontiers in pharmacology, 11: 586993.

Osipiuk J, Azizi SA, Dvorkin S, Endres M, Jedrzejczak R, Jones KA, Kang S, Kathayat RS, Kim Y, Lisnyak VG, Maki SL, Nicolaescu V, Taylor CA, Tesar C, Zhang YA, Zhou Z, Randall G, Michalska K, Snyder SA, Dickinson BC, Joachimiak A, 2021. Structure of papain-like protease from SARS-CoV-2 and its complexes with non-covalent inhibitors. Nature communications, 12(1): 743.

Parga-Lozano C, 2020. Hibiscus Sabdariffa como candidato terapéutico para COVID-19. Duazary, 17(4): 1-3.

Shawky E, Nada AA, Ibrahim RS, 2020. Potential role of medicinal plants and their constituents in the mitigation of SARS-CoV-2: identifying related therapeutic targets using network pharmacology and molecular docking analyses. RSC Advances, 10(47): 27961-27983.

Singh G, Pawan, Mohit, Diksha, Suman, Priyanka, Sushma, Saini A, Kaur A, 2022. Design of new bis-triazolyl structure for identification of inhibitory activity on COVID-19 main protease by molecular docking approach. Journal of molecular structure, 1250: 131858.

Solnier J, Fladerer JP, 2021. Flavonoids: A complementary approach to conventional therapy of COVID-19? Phytochemistry reviews : proceedings of the Phytochemical Society of Europe, 20(4): 773-795.

Steklac M, Zajacek D, Bucinsky L, 2021. 3CL(pro) and PL(pro) affinity, a docking study to fight COVID19 based on 900 compounds from PubChem and literature. Are there new drugs to be found? Journal of molecular structure, 1245: 130968.

Takeuchi Y, Akashi Y, Kato D, Kuwahara M, Muramatsu S, Ueda A, Notake S, Nakamura K, Ishikawa H, Suzuki H, 2021. The evaluation of a newly developed antigen test (QuickNavi-COVID19 Ag) for SARS-CoV-2: A prospective observational study in Japan. Journal of infection and chemotherapy : official journal of the Japan Society of Chemotherapy, 27(6): 890-894.

Tomani JCD, Kagisha V, Tchinda AT, Jansen O, Ledoux A, Vanhamme L, Frederich M, Muganga R, Souopgui J, 2020. The Inhibition of NLRP3 Inflammasome and IL-6 Production by Hibiscus noldeae Baker f. Derived Constituents Provides a Link to Its Anti-Inflammatory Therapeutic Potentials. Molecules, 25(20).

Vlachakis D, Papakonstantinou E, Mitsis T, Pierouli K, Diakou I, Chrousos G, Bacopoulou F, 2020. Molecular mechanisms of the novel coronavirus SARS-CoV-2 and potential anti-COVID19 pharmacological targets since the outbreak of the pandemic. Food and chemical toxicology : an international journal published for the British Industrial Biological Research Association, 146: 111805.

WHO, 2022. COVID-19 Therapeutics under Assessment.

Wu C, Liu Y, Yang Y, Zhang P, Zhong W, Wang Y, Wang Q, Xu Y, Li M, Li X, Zheng M, Chen L, Li H, 2020. Analysis of therapeutic targets for SARS-CoV-2 and discovery of potential drugs by computational methods. Acta pharmaceutica Sinica. B, 10(5): 766-788.